Ultrasonic Velocity and Absorption in $(Li,Ag)NO_3$, $(Na,Ag)NO_3$, $(K,Ag)NO_3$, $(Cs,Ag)NO_3$, $(Li,Rb)NO_3$, and $(Na,Rb)NO_3$ Melts Measured by the Pulse Transmission Method

E. Rejek, J. Richter, A. Stark, and M. Vogt

Institut für Physikalische Chemie der RWTH Aachen, Aachen

Z. Naturforsch. **49a**, 481–489 (1994); received November 15, 1993

Ultrasonic velocity and absorption have been measured in molten $(Li,Ag)NO_3$, $(Na,Ag)NO_3$, $(K,Ag)NO_3$, $(Cs,Ag)NO_3$, $(Li,Rb)NO_3$, and $(Na,Rb)NO_3$ as functions of composition in the temperature range 230 to 300 °C. An improved pulse transmission device was applied. The obtained accuracy was 2‰ for the velocity and 2–4% for the absorption data. The ultrasonic velocity and absorption coefficient (25 MHz) were found to depend linearly on temperature. The dependence of the velocity on the mole fraction could be represented by a cubic polynomial. For the absorption values (referred to the square of frequency) a reasonable general dependence on composition could not be given. The adiabatic compressibility of all mixtures has been calculated from the measured sound velocity. The ratio bulk/shear viscosity and the bulk viscosity itself follow from the measured absorption values together with the velocity values. The conclusion from these data is that ultrasonic absorption in the six investigated systems is governed by the bulk viscosity and that structural rearrangements rather than structural relaxation of the molecules, are the reason for high bulk viscosities in ionic melts.

Key words: Molten salts, Thermophysical properties, Ultrasonic velocities and absorption, Pulse transmission method.

Introduction

The sound velocity u in a liquid is governed by the adiabatic compressibility $\varkappa_s$,

$$u^2 = \frac{1}{\varrho_0 \varkappa_s}, \tag{1}$$

where ϱ_0 denotes the density of the undisturbed liquid. The attenuation of the sound wave is given by $I_x = I_0 \exp(-2\alpha x)$, where I_x is the sound intensity at position x and α the (amplitude) absorption coefficient. According to non-equilibrium thermodynamics [1]

$$\alpha = \frac{\omega^2}{2\varrho_0 u^3}\left[\frac{4}{3}\eta + \eta' + \frac{\lambda'(\gamma-1)}{\tilde{c}_P}\right], \tag{2}$$

where $\omega/(2\pi)$ is the sound frequency f, η the shear viscosity, λ' the thermal conductivity (the prime distinguishes it from wavelength), γ the adiabatic constant, and $\tilde{c}_P$ the specific isobaric heat capacity. The bulk (or volume) viscosity η' is a measure of the friction experienced in a pure expansion or compression. In molten salts the bulk viscosity may exceed the shear viscosity by an order of magnitude, and the attenuation by the shear viscosity is one or two orders of magnitudes larger than that by thermal conductivity. Thus, for molten salts the attenuation by thermal conductivity can be neglected.

The relation between u and α is provided by the linear response theory, according to which both u and α – including their frequency dependences – can be reduced to one real time correlation function. This formalism is not discussed in this experimental paper.

The classical viscothermal theory [2, 3] does not contain the bulk viscosity so that the classical absorption coefficient α_{class} can be calculated from the ultrasonic velocity, measured in this paper, and by literature values of ϱ_0 and η [4]. From (2) and α_{class} it follows that

$$\frac{\eta'}{\eta} = \frac{4}{3}\left(\frac{\alpha}{\alpha_{class}} - 1\right). \tag{3}$$

Experimental

The experiments have been carried out with a pulse transmisson device adapted for measurements in molten salts at higher temperatures. In this method

Reprint requests to Prof. Dr. J. Richter, Institut für Physikalische Chemie, Technische Hochschule Aachen, Templergraben 59, D-52056 Aachen.

0932-0784 / 94 / 0300-0481 $ 01.30/0. – Please order a reprint rather than making your own copy.

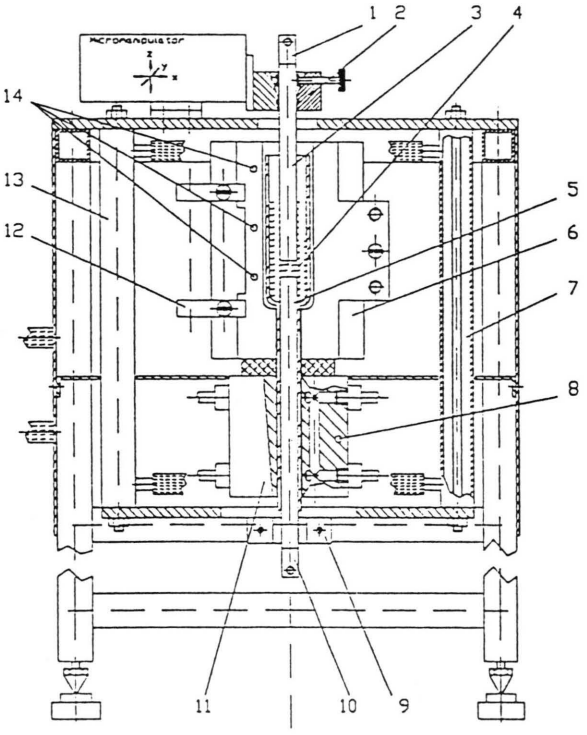

1	Transmitter	7, 13	Equilibrated Distance Controller
2, 9	Mounting Plates	8, 14	Thermocouple
3, 5	Quartz Rods	10	Receiver
4	Measuring Cell	11	Cooling System
6	Heating Plates	12	Stainless Steel Block

Fig. 1. Sectional view of the pulse transmission device.

the sound absorption is evaluated from the change of the amplitude of ultrasonic pulses passing a variable but defined distance through the melt. The sound velocity is calculated from the transit time of the signal.

The experimental set-up is shown in Figure 1. The molten salt is contained in a Duran-glass cell. Two quartz rods enter the vessel from above and from below. The sealing between the vessel and the lower quartz rod is performed by the salt itself, solidifying in the region of the cooling system (No. 11 in Figure 1). Transmitting quartzes are mounted at the open ends of the quartz rods. The quartz rods are required to separate the piëzoelectric quartz transducers, which are sensitive to temperature, from the melt at about 300 °C. These transducers can be used both as transmitters and receivers. The measuring cell is placed in a spliced block of massive stainless steel with heating resistors on the outer surface held by aluminium plates. A 5 cm layer of fibre glass like material (FG 7, Bulthen-Kanthal) is used for thermal insulation.

The apparatus is essentially improved, and the volume of the furnace is 75% smaller compared to the one used in [5]. The temperature errors amount to about 0.25 K in the cover of the furnace and to about 0.1 K in the melt. The lower quartz rod, together with the cell, is held in a PVC-mounting on a bracket below the furnace. The upper quartz rod is positioned in an adjustable aluminium block, which is held by a micromanipulator type HS 6 (Bachofer GmbH). Thus the inclination of the upper rod can be precisely adjusted so that the front sides of the transmitter and the receiver are parallel. The micromanipulator has a resolution of 1 μm and allows a precise control of the upper quartz rod in the three space coordinates. So both rods can be aligned to minimize measuring errors in the sound intensity. The mounting plate of the lower quartz rod is connected only to the frame of the apparatus at the equilibrated support. In that way the distance between the upper and lower piëzoelectric quartz is maintained stationary even in case of thermal variations in the set-up, so that errors in the distance determination are reliably avoided.

The electric and electronic periphery is divided into two groups supplied by separate power lines: One consists of units which are insensitive to voltage fluctuations or have a high power consumption like the transformer, controller, and thermostat. The other group is formed by the sensitive measurement equipment. Square wave modulated high frequency pulses (3 V at 50 Ω, 10–35 MHz, 1 μs duration) are generated by a signal generator and modulated by a pulse generator. The pulses detected by the receiver are attenuated by about 80 dB compared to the transmitted pulses and they are delayed by about 50 μs. After amplification to 7–9 V and demodulation the signal is sent to a voltmeter as well as to one channel of a dual beam oscilloscope. The oscilloscope is triggered by the signal of the pulse generator. By setting its delay marker to the maximum of the received signal the oscilloscope generates a trigger pulse which is used to sample the received signal by the voltmeter at the right time. A computer reads this digitized value via an IEEE-bus from the voltmeter. The distance between the two transmitting quartzes is automatically varied in well-defined steps by the micrometer drive mechanism. The corresponding amplitudes of the signals are recorded over a total distance of 20 mm. The absorption coefficient results from the attenuation at each

tested distance. The sound velocity results from the transit time between transmitted and received pulses, which is measured with an accuracy of 10 μs by the oscilloscope.

Results

The ultrasonic velocity and absorption of six binary nitrate melts were measured as a function of mole fraction at four different temperatures. The frequency of all measurements was 25 MHz. Average values of u and α at each composition and standard deviations were formed on the basis of five to eight measurements.

The ultrasonic velocities depending on composition at four temperatures are plotted for the systems $(Li,Ag)NO_3$, $(Na,Ag)NO_3$, $(K,Ag)NO_3$, $(Cs,Ag)NO_3$, $(Li,Rb)NO_3$, $(Na,Rb)NO_3$ in Figs. 2–7, respectively. The data of Figs. 3 and 4 complete earlier ones [5], and the data of Fig. 5 are of higher accuracy than those measured earlier by the Debye-Sears method [6]. The velocity decreases from pure $LiNO_3$, $NaNO_3$, and KNO_3, respectively, to the value of pure silver nitrate by about 200 ms^{-1}. In $(Rb,Ag)NO_3$ [5] u goes down to a minimum and increases again nearly to the value of pure $AgNO_3$. In $(Cs,Ag)NO_3$ u increases from $CsNO_3$ to $AgNO_3$ by about 200 ms^{-1}. In $(Li,Rb)NO_3$ and $(Na,Rb)NO_3$ the velocity drops again by about 200 ms^{-1} going from $LiNO_3$ and $NaNO_3$ to $RbNO_3$, respectively. The error bars in the figures correspond to the 2σ-interval, e.g. a confidence interval of 99%. The values of Higgs and Litovitz [7] at 55–125 MHz for pure $LiNO_3$ and $AgNO_3$ fit well into the curves, as do the values of Cerisier et al. [8] at 100 kHz for pure silver nitrate at the four measured temperatures and for pure lithium nitrate in both systems.

The temperature dependence of the sound velocity is linear in all six mixtures: $u = a_0 - a_1 T_C$, where T_C denotes the Celsius temperature; a_0 (ms^{-1}), a_1 ($ms^{-1} K^{-1}$) are fit coefficients, which are given for constant mole fraction in Table 1 if the temperature covers a range of 70 K. The mole fraction dependence of the sound velocity can be represented by the polynomial $u(x_i)/u^+ = b_0 + b_1 x_i + b_2 x_i^2 + b_3 x_i^3$ with an accuracy better than 2.5‰. T_C is constant, $u^+ \equiv 1\ ms^{-1}$, $x_i = x_{AgNO_3}$ or x_{RbNO_3}. The fit coefficients b_j, together with the standard deviations s_1, are listed in Table 2 for the six systems at 300 °C.

The results of the absorption coefficients for the six systems are summarized in Table 3. In Figs. 8 and 9, αf^{-2} at 300 °C is plotted versus x_{AgNO_3} and x_{RbNO_3} respectively. The data of the systems $(Na,Ag)NO_3$, $(K,Ag)NO_3$, and $(Cs,Ag)NO_3$ are updated values, now all measured by the pulse transmission method with much higher precision than the previous ones [5, 6]. In the system $(Li,Ag)NO_3$ the composition dependent product αf^{-2} decreases from pure silver nitrate, attains a minimum and then increases slowly towards pure $LiNO_3$. The values given by Higgs and Litovitz [7] just fit into the curve within the measuring accuracy, as plotted in Figure 8. In $(Na,Ag)NO_3$ the

Table 1. Sound velocities: Coefficients of the balancing equation $u = a_0 - a_1 T_C$ of the six system.

x_{AgNO_3}	$(Li,Ag)NO_3$		$(Na,Ag)NO_3$		$(K,Ag)NO_3$		$(Cs,Ag)NO_3$		x_{RbNO_3}	$(Li,Rb)NO_3$		$(Na,Rb)NO_3$	
	a_0 / ms^{-1}	a_1 / $ms^{-1}K^{-1}$	a_0 / ms^{-1}	a_1 / $ms^{-1}K^{-1}$	a_0 / ms^{-1}	a_1 / $ms^{-1}K^{-1}$	a_0 / ms^{-1}	a_1 / $ms^{-1}K^{-1}$		a_0 / ms^{-1}	a_1 / $ms^{-1}K^{-1}$	a_0 / ms^{-1}	a_1 / $ms^{-1}K^{-1}$
0.30									0.3	1968.4	1.10		
0.35	1844.1	0.79			2025.8	1.29							
0.40	1838.7	0.80			2007.1	1.27			0.4	1973.2	1.20	2074.7	1.38
0.45	822.7	0.79			2000.9	1.31	1666.7	1.07					
0.50	1822.7	0.82			1935.3	1.12	1675.8	1.08	0.5	1956.9	1.21	2048.6	1.37
0.55	1819.6	0.84			1923.0	1.16	1688.8	1.10					
0.60	825.0	0.89			1912.6	1.19	1693.4	1.08	0.6	1964.1	1.29	2003.7	1.32
0.65	1816.4	0.88			1893.5	1.16	1700.0	1.06					
0.70	1815.6	0.89			1878.8	1.14	1686.0	0.96	0.7	1960.2	1.33		
0.75	1824.6	0.93			1871.7	1.16	1732.6	1.08					
0.80	1813.0	0.92	1845.3	1.00	1845.6	1.07	1744.9	1.06	0.8	1926.7	1.26		
0.85	1819.4	0.95	1827.1	0.97	1838.9	1.06	1751.8	1.01					
0.90	1814.9	0.94	1826.0	0.98	1826.7	1.02	1783.2	1.04					
0.95	815.1	0.95	1814.0	0.95	1820.2	1.00	1793.8	0.99					
1.00	1819.7	1.00	1819.7	1.00	1819.7	1.00	1819.7	1.00					

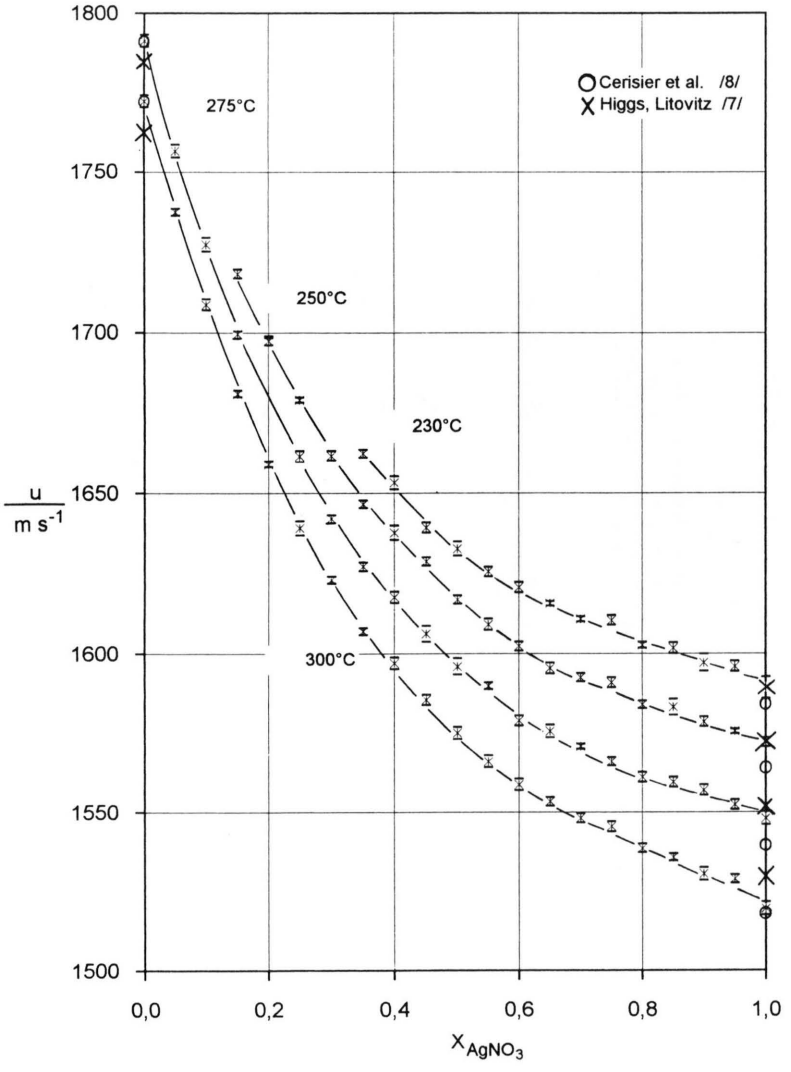

Fig. 2. Ultrasonic velocity in $(Li,Ag)NO_3$ as a function of the mole fraction of silver nitrate at different temperatures.

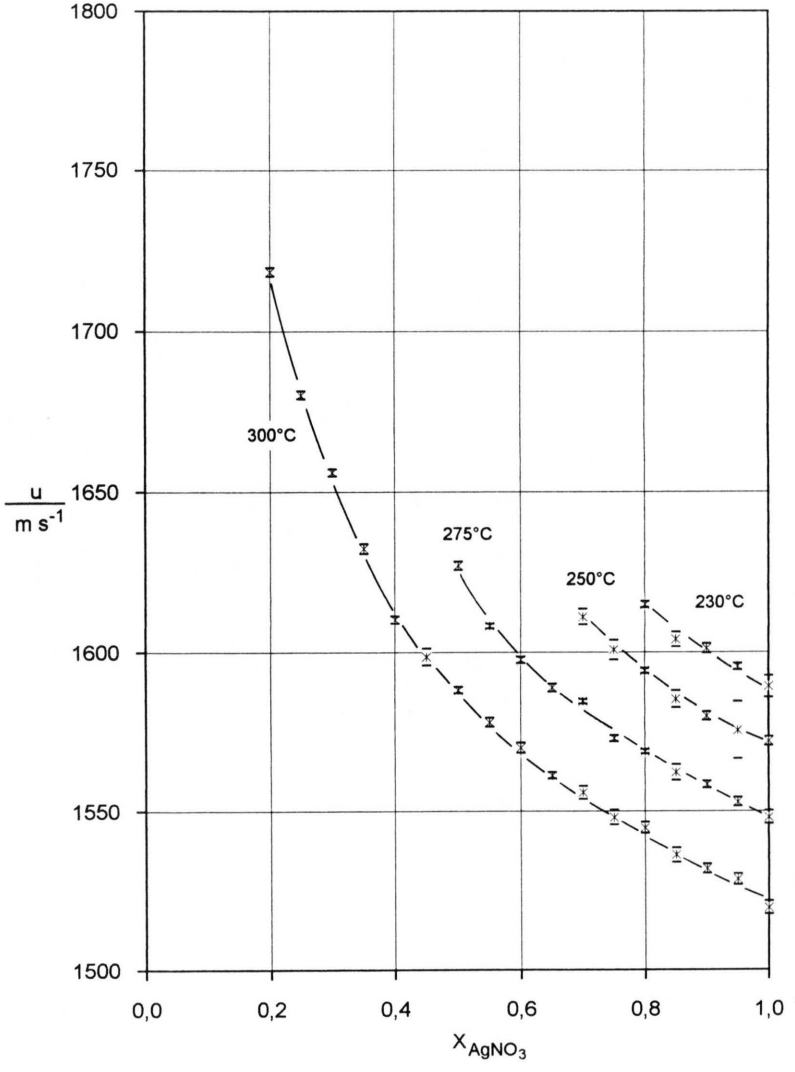

Fig. 3. Ultrasonic velocity in $(Na,Ag)NO_3$ as a function of the mole fraction of silver nitrate at different temperatures.

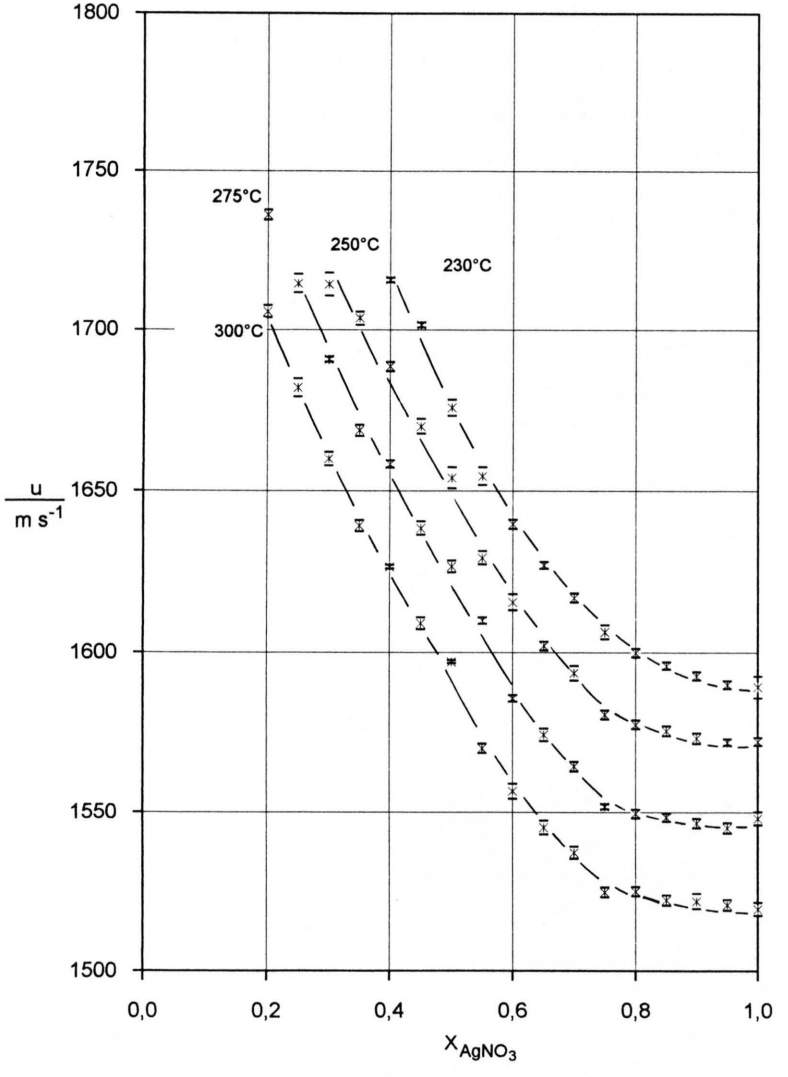

Fig. 4. Ultrasonic velocity in $(K,Ag)NO_3$ as a function of the mole fraction of silver nitrate at different temperatures.

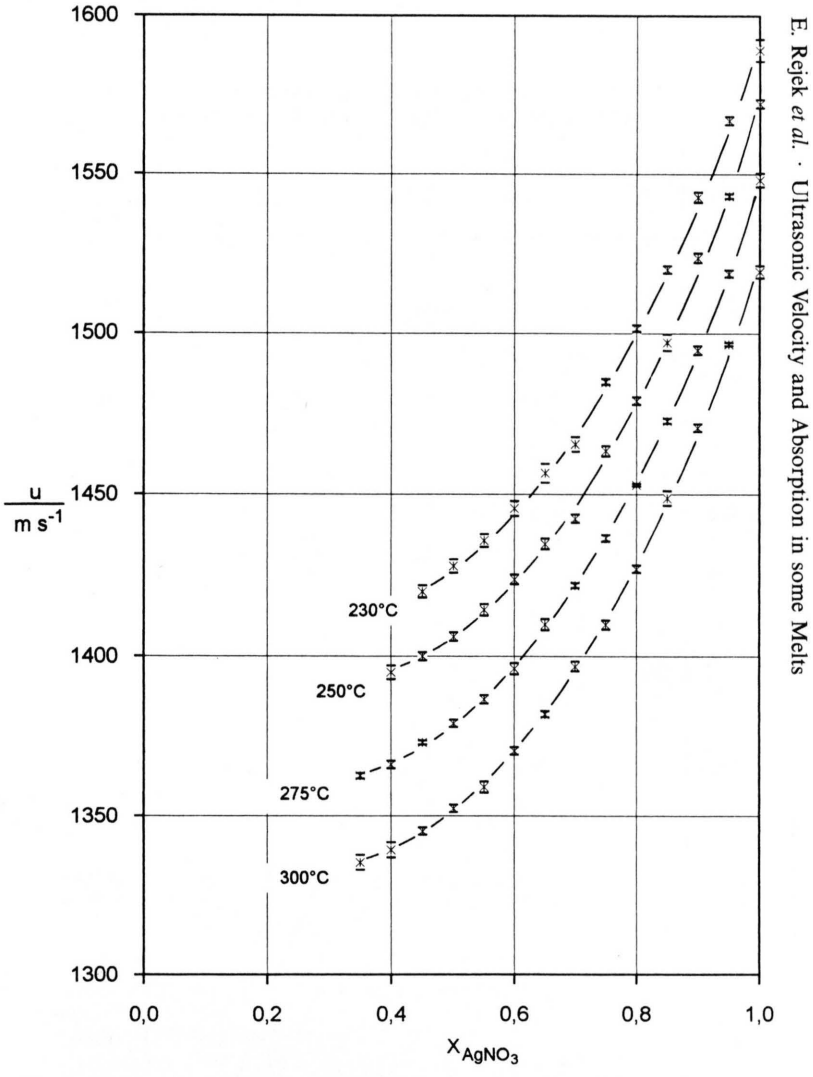

Fig. 5. Ultrasonic velocity in $(Cs,Ag)NO_3$ as a function of the mole fraction of silver nitrate at different temperatures.

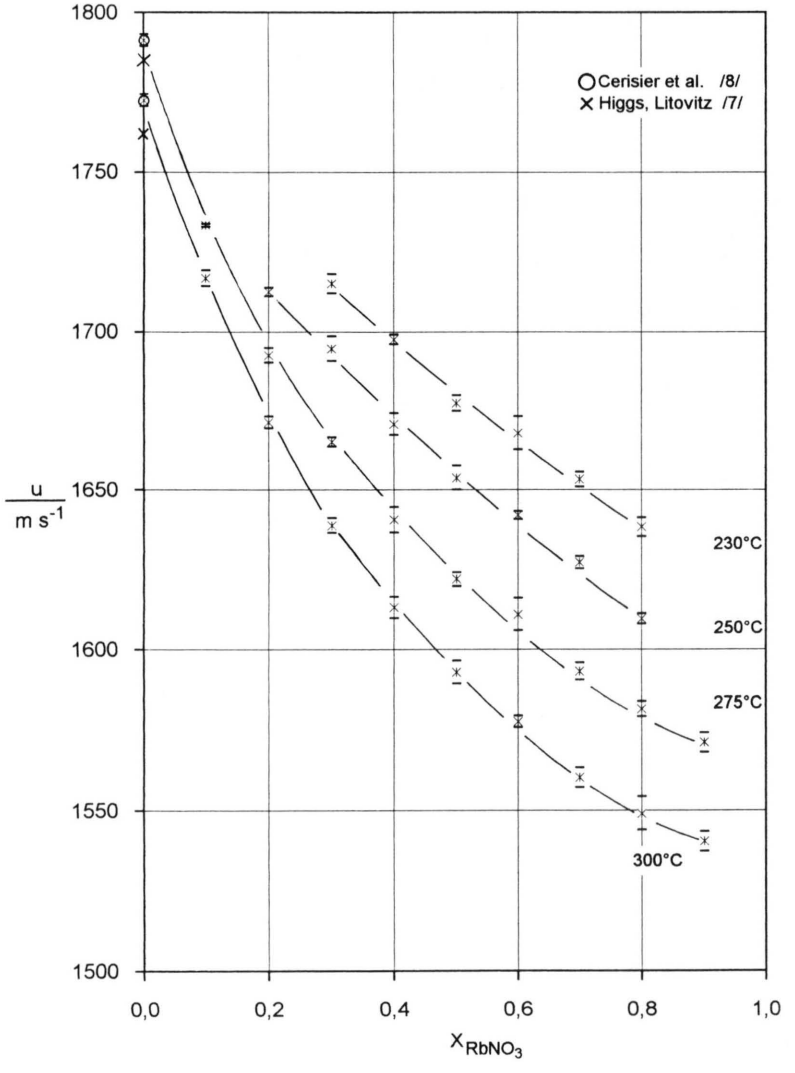

Fig. 6. Ultrasonic velocity in $(Li,Rb)NO_3$ as a function of the mole fraction of rubidium nitrate at different temperatures.

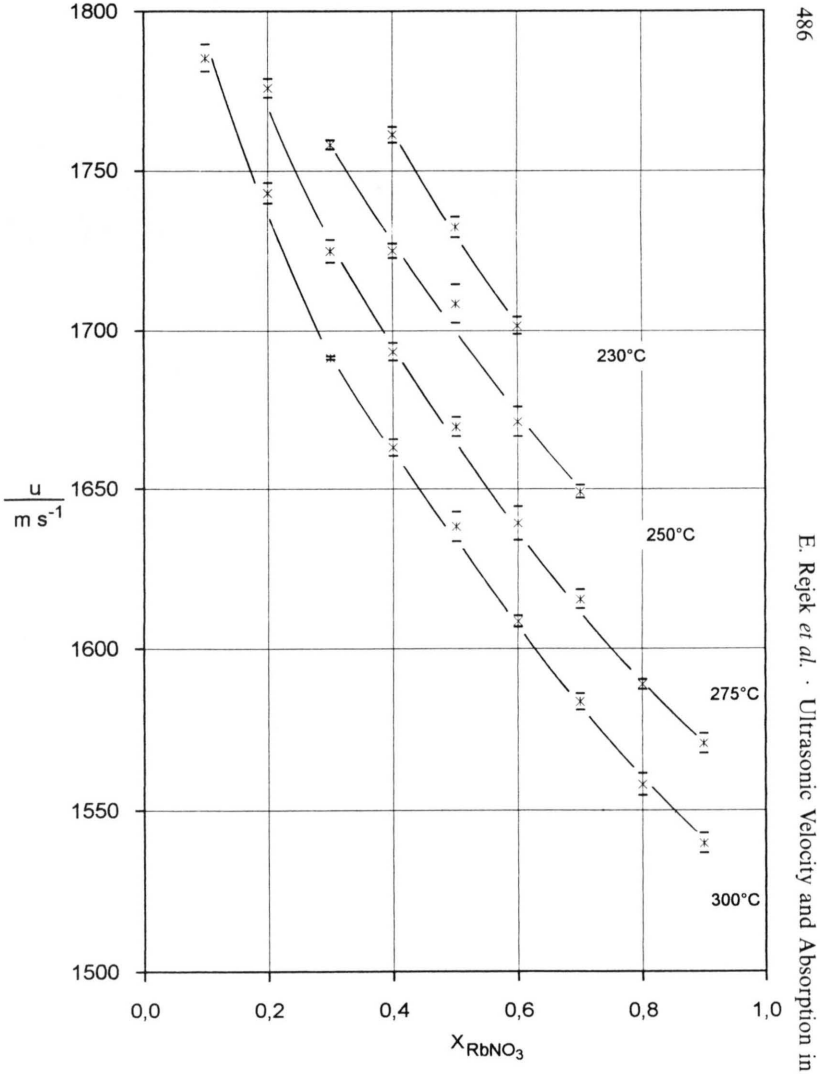

Fig. 7. Ultrasonic velocity in $(Na,Rb)NO_3$ as a function of the mole fraction of rubidium nitrate at different temperatures.

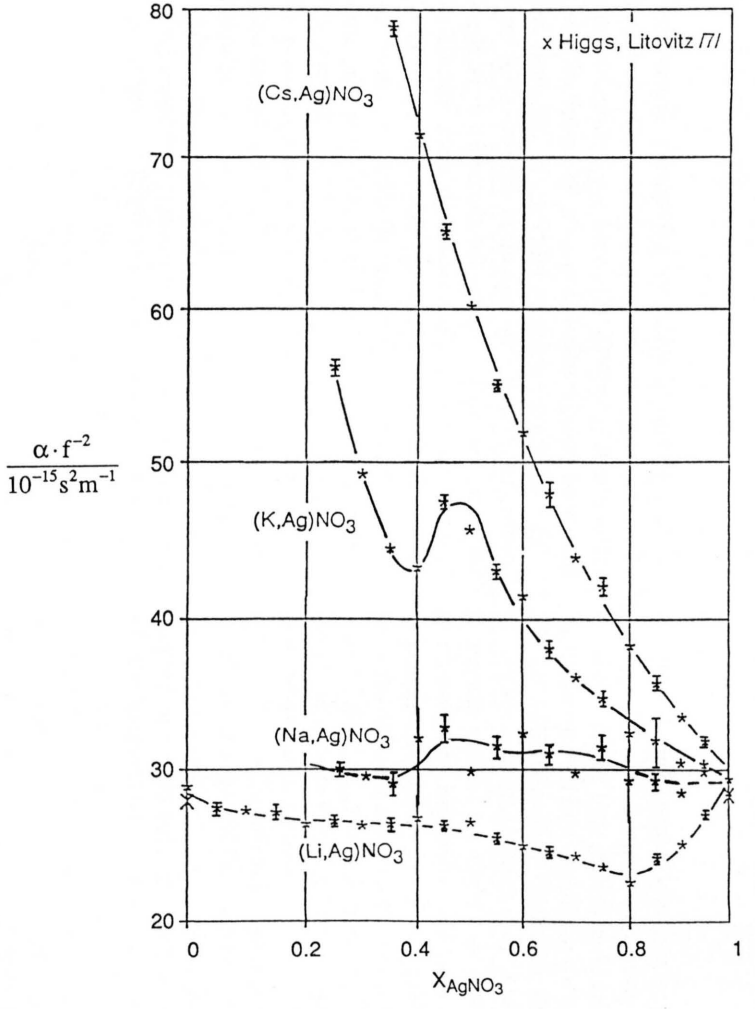

Fig. 8. Ultrasonic absorption in $(M,Ag)NO_3$ as a function of the mole fraction of silver nitrate at 300 °C.

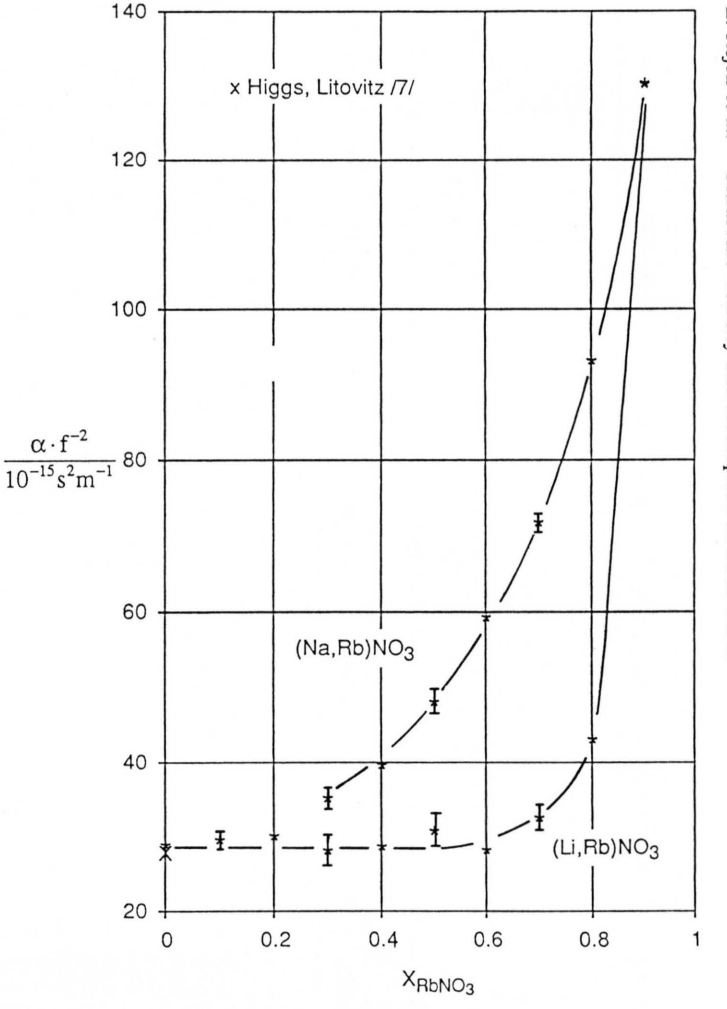

Fig. 9. Ultrasonic absorption in $(Li,Rb)NO_3$ and $(Na,Rb)NO_3$ as a function of the mole fraction of rubidium nitrate at 300 °C.

Table 2. Coefficients of the equation $u = b_0 + b_1 x_i + b_2 x_i^2 + b_3 x_i^3$ and standard deviations s_1 for the six systems at 300 °C.

	$(Li,Ag)NO_3$	$(Na,Ag)NO_3$	$(K,Ag)NO_3$	$(Cs,Ag)NO_3$	$(Li,Rb)NO_3$	$(Na,Rb)NO_3$
b_0	1770.7	1897.0	1823.3	1370.4	1771.5	1842.7
b_1	−693.2	−1163.6	−640.4	−227.9	−605.3	−611.5
b_2	759.0	1383.1	336.2	377.3	623.7	493.5
b_3	−316.1	−597.4	0	0	−265.1	−211.1
s_1	1.4	2.5	4.5	1.5	1.9	4.4

Table 3. Sound absorption: Coefficients c_0 [in $10^{-15}\,s^2\,m^{-1}$] and c_1 [in $10^{-15}\,s^2\,K\,m^{-1}$] of the balancing equation $\alpha f^{-2} = c_0 - c_1 T_C$ of the six systems.

x_{AgNO_3}	$(Li,Ag)NO_3$		$(Na,Ag)NO_3$		$(K,Ag)NO_3$		$(Cs,Ag)NO_3$		x_{RbNO_3}	$(Li,Rb)NO_3$		$(Na,Rb)NO_3$	
	c_0	c_1	c_0	c_1	c_0	c_1	c_0	c_1		c_0	c_1	c_0	c_1
									0.30	76.6	0.16		
0.35	64.0	0.13			85.7	0.14							
0.40	57.7	0.10			92.5	0.17			0.40	78.9	0.17	98.9	0.20
0.45	55.5	0.10			79.7	0.11	111.0	0.16					
0.50	53.3	0.09			75.5	0.10	102.0	0.14	0.50	80.7	0.17	115.5	0.23
0.55	54.1	0.10			68.2	0.09	97.9	0.14					
0.60	51.1	0.09			65.4	0.08	90.0	0.13	0.60	88.4	0.20	116.1	0.20
0.65	52.8	0.09			68.8	0.10	84.0	0.12					
0.70	52.0	0.09			69.4	0.11	81.9	0.13	0.70	86.6	0.19		
0.75	52.2	0.10			67.5	0.11	70.2	0.10					
0.80	53.7	0.11	50.6	0.07	68.5	0.12	70.3	0.11	0.80	103.2	0.21		
0.85	46.1	0.08	52.3	0.08	56.8	0.08	65.6	0.10					
0.90	44.1	0.06	53.8	0.08	63.8	0.11	63.1	0.10					
0.95	46.4	0.07	52.2	0.08	59.9	0.10	59.6	0.09					
1.00	58.4	0.10	58.4	0.10	58.4	0.10	58.4	0.10					

sound absorption is virtually independent of composition within the given error bars. In the $(K,Ag)NO_3$ mixture αf^{-2} increases rapidly and passes – outside the limits of error – a maximum and then a minimum, which have been measured quite carefully. In the system $(Cs,Ag)NO_3$ one finally gets a steep rise of αf^{-2} from $AgNO_3$ to $CsNO_3$; it is even steeper in the system $(Na,Rb)NO_3$ when the composition is varied from $NaNO_3$ to $RbNO_3$ (Fig. 9), whereas in $(Li,Rb)NO_3$ the sound absorption remains constant from the $LiNO_3$ side up to about $x_{RbNO_3} = 0.7$, where it steeply increases up to five times this value. However, this value might have some uncertainty because it is very close to the liquidus curve.

No fit which is valid for all six systems could be found for the dependence of the absorption constants on the mole fraction. However, the temperature dependence can always be represented by $\alpha f^{-2} = c_0 + c_1 T_C$. Table 3 contains these fit coefficients again for those mole fractions where the temperature covers a range of 70 K. In many cases measurements were performed in a frequency range between 10 and 50 MHz, but a frequency dependence of sound absorption as observed by the Debye-Sears method in $(Cs,Ag)NO_3$ [6] could not be found by the improved pulse transmission method described here.

The adiabatic compressibility $\varkappa_s$, as obtained according to (1) using the measured ultrasonic velocity values and literature values for the densities [4, 9], is listed in Table 4. $\varkappa_s$ decreases from alkali nitrate to pure silver nitrate in all $(M,Ag)NO_3$ systems at 300 °C (M = Li, Na, K, Cs). In the $(Li,Rb)NO_3$ system $\varkappa_s$ remains nearly constant, and in the $(Na,Rb)NO_3$ mixture it increases slightly from $NaNO_3$ to $RbNO_3$.

The ratio of bulk viscosity η' to shear viscosity η, as obtained from (2) and (3) is listed in Table 4 along with the bulk viscosity itself. The ratio η'/η varies between 6 and 13; i.e. the bulk viscosity in the (alkali, rubidium) nitrate mixtures rich in $RbNO_3$ is thirteen times larger than the shear viscosity. In $(Li,Ag)NO_3$ and $(Na,Ag)NO_3$ mixtures the bulk viscosity increases with increasing silver nitrate mole fraction, but decreases with increasing x_{AgNO_3} in $(K,Ag)NO_3$ and $(Cs,Ag)NO_3$. In $(K,Ag)NO_3$ η' of pure silver nitrate

Table 4. Adiabatic compressibility [in 10^{-10} s^2 m kg^{-1}], ratio bulk viscosity/shear viscosity, and bulk viscosity [in 10^{-3} kg s^{-1} m^{-1}] of the six systems at 300 °C.

x_{AgNO_3}	(Li,Ag)NO_3			(Na,Ag)NO_3			(K,Ag)NO_3			(Cs,Ag)NO_3			x_{RbNO_3}	(Li,Rb)NO_3			(Na,Rb)NO_3		
	$\varkappa_s$	η'/η	η'	$\varkappa_s$	η'/η	η'	$\varkappa_s$	η'/η	η'	$\varkappa_s$	η'/η	η'		$\varkappa_s$	η'/η	η'	$\varkappa_s$	η'/η	η'
0.0	1.80	2.06	8.72										0.0	1.80	2.06	8.72			
0.1	1.71	2.14	8.46										0.1	1.82	2.22	8.81	1.58	5.23	16.65
0.2	1.64	2.30	8.56										0.2	1.83	2.41	8.95	1.60	5.04	16.13
0.3	1.55	2.65	9.24	1.46	4.37	12.95	1.51	7.36	23.20				0.3	1.81	2.17	7.94	1.65	3.92	13.61
0.4	1.47	3.20	10.37	1.44	4.68	14.08	1.46	6.71	20.30	1.73	6.76	23.37	0.4	1.80	2.28	8.19	1.65	4.04	15.17
0.5	1.40	3.65	11.01	1.38	4.35	13.31	1.41	7.64	22.27	1.66	6.48	20.62	0.5	1.78	2.65	9.25	1.66	5.19	19.10
0.6	1.33	3.55	10.71	1.32	5.18	15.51	1.39	6.90	19.74	1.57	6.11	18.80	0.6	1.76	2.28	8.05	1.67	6.64	23.97
0.7	1.27	3.62	10.93	1.26	5.00	14.65	1.33	6.23	17.44	1.47	5.77	17.15	0.7	1.75	2.65	9.76	1.69	7.62	29.00
0.8	1.21	3.49	10.46	1.21	5.23	15.09	1.26	5.83	16.13	1.36	5.65	16.39	0.8	1.74	3.67	14.23	1.70	9.43	37.73
0.9	1.16	4.39	12.83	1.16	5.29	15.16	1.19	5.82	16.04	1.24	5.66	16.26	0.9	1.72	13.23	53.61	1.71	13.04	54.84
1.0	1.12	5.77	16.39	1.12	5.77	16.39	1.12	5.99	16.48	1.12	5.77	16.39	1.0						

deviates from the value in the other systems due to more recent shear viscosity data [10]. In the two (alkali, rubidium) nitrate mixtures the increasing tendency of η' with the mole fraction of rubidium nitrate is much more pronounced than in the (alkali, silver) nitrate mixtures. The plots of η' versus mole fraction show the same characteristic dependence on composition as αf^{-2}. Therefore we can conclude that the ultrasound absorption in the six investigated systems is governed by η'. The temperature coefficient of the bulk viscosity is clearly negative for all mixtures. In an Arrhenius plot the temperature dependence of η' is nearly linear for the (Li,Ag)NO_3, (Na,Ag)NO_3, and (Cs,Ag)NO_3 mixtures; in (K,Ag)NO_3, (Li,Rb)NO_3, and (Na,Rb)NO_3 there are obvious deviations from the Arrhenius behaviour. Together with the above mentioned variation of the η'/η ratio it follows from the Kneser theory [11] that structural rearrangements rather than structural relaxation of the molecules, are responsible for the high bulk viscosity and thus for the ultrasonic absorption in ionic melts. In total, the precision of the absorption data of molten salts has been improved by employing the pulse transmission method used also in [5]. When applied to molten salts, the pulse transmission method is now more accurate than the Debye-Sears method. This explains the deviations of our present data from the data published earlier in this journal [5, 6] and may hopefully be of value for the development and testing of a more general picture of transport properties in molten salts.

Acknowledgement

Financial support by the Bundesministerium für Forschung und Technologie (BMFT) through the Deutsche Agentur für Raumfahrtangelegenheiten DARA (Förderkennzeichen 01 QV 8949), and by the Minister für Wissenschaft und Forschung des Landes Nordrhein-Westfalen is gratefully acknowledged.

[1] S. R. de Groot and P. Mazur, Non-equilibrium Thermodynamics, North Holland Publishing Company, Amsterdam 1962.
[2] G. G. Stokes, Cambridge Transaction **8,** 287 (1845).
[3] G. Kirchhoff, Pogg. Ann. **134,** 177 (1868).
[4] G. J. Janz, U. Krebs, H. F. Siegenthaler, and R. P. T. Tomkins, J. Phys. Chem. Ref. Data **1,** 581 (1972).
[5] W. Fuchs and J. Richter, Z. Naturforsch. **39a,** 1279 (1984).
[6] J. Richter and B. Fuchs, Z. Naturforsch. **41a,** 535 (1986).
[7] R. W. Higgs and T. A. Litovitz, J. Acoust. Soc. Amer. **32,** 1108 (1960).
[8] P. Cerisier, G. Finiels, and Y. Doucet, J. Chim. Phys. **71,** 836 (1974).
[9] NIST Std. Ref. Database 27; NIST Properties of Molten Salts 3½″ DD, US Dept. of Commerce 1992.
[10] A. Schardey, J. Richter, and H. A. Øye, Ber. Bunsenges. Phys. Chem. **92,** 64 (1988).
[11] H. O. Kneser, Ann. Physik **32,** 277 (1939).